Development of thermoresponsive poly(propylene-*g*-*N*-isopropylacrylamide) non-woven 3D scaffold for smart cell culture using oxyfluorination-assisted graft polymerisation

Avashnee S. Chetty[a*], Viktoria Vargha[b], Arjun Maity[a], F. Sean Moolman[a], Claire Rossouw[c], Rajesh Anandjiwala[a], Lydia Boguslavsky[a], Dalu Mancama[c], and Walter W. Focke[d]

[a] Materials Science and Manufacturing, CSIR, PO Box 395, Pretoria 0001, South Africa
[b] Department of Physical Chemistry and Material Science, Budapest University of Technology and Economics, Műegyetem rkp. 3. H/1, Budapest H-1111, Hungary [c] CSIR Biosciences, CSIR, PO Box 395, Pretoria 0001, South Africa
[d] Institute of Applied Materials, University of Pretoria, Pretoria 0001, South Africa

Corresponding author: telephone: +27-12-841-3239; fax: +27-12-841-3553; e-mail:

achetty@csir.co.za (A Chetty)

ABSTRACT

Growing cells on 3D scaffolds is far superior to the conventional 2D monolayer culture method. In this study, a novel 3D thermoresponsive poly(propylene-*g*-*N*-isopropylacrylamide) (PP-*g*-PNIPAAm) non-woven fabric (gNWF) was developed for cell culture using oxyfluorination-assisted graft polymerisation (OAGP). New polar functional groups were detected on the oNWF, and PNIPAAm was confirmed in the gNWF by Attentuated Total-Reflectance Fourier transform infrared (ATR-FTIR) and scanning x-ray photoelectron spectroscopy (S-XPS). Scanning electron microscopy (SEM) revealed a rough surface morphology and confinement of the PNIPAAm graft layer to the surface of the fibres in the gNWF. The OAGP method did not affect the crystalline phase of bulk PP, however, twin-melting thermal peaks were detected for the oNWF and gNWF indicating crystal defects. Contact angle studies showed that the surface of the gNWF exhibited a thermoresponsive behaviour. Hepatocyte cells attached onto gNWF disks in a bioreactor at 37°C and remained viable for 10 days in culture. Upon cooling the cell culture media to 20°C, cells were spontaneously released as 3D multi-cellular constructs without requiring destructive enzymes. The development of 3D thermoresponsive scaffolds capable of non-invasive 3D cell culture could provide a more reliable *in vitro* model for cells.
Keywords: Oxyfluorination; graft polymerisation; surface functionalisation; poly(propylene) (PP); Poly(N-isopropylacrylamide)

1. Introduction

It is well-known that cells grown onto 3D surfaces show closer similarities to their *in vivo* counterparts in terms of cell morphologies, behaviour, and function than 2D surfaces[1,2]. A

major limitation of existing 3D scaffolds however is that they rely on destructive means to release the proliferated cells. These include enzymatic digestion of the extracellular matrix (ECM), mechanical scraping of the cells, or chemical degradation of the matrix. Such release mechanisms cause irreversible damage to cells leading to disruptions in essential receptor-ligand interactions on the cell surface [3]. Damage to the ECM is known to adversely influence cell signalling pathways which affect important cell processes such as adhesion, proliferation, differentiation, migration, structure, and gene expression [4]. Furthermore, concerns exist with regards to the animal origin of some of the 3D ECM scaffolds and the associated production variability [1]. This, combined with the additional wash steps and extra handling requirements, results in high costs, well-to-well variations, and culture inconsistencies.

Poly(*N*-isopropylacrylamide) (PNIPAAm), a temperature responsive polymer, has revolutionised the cell culture fraternity by providing a non-invasive means of harvesting adherent cells, whereby confluent cells can be spontaneously released by simply cooling the cell culture medium and without requiring enzymes. The pioneering work by Okano *et al* [5] showed that cells could be released as intact monolayer cell sheets from the surface of PNIPAAm coated tissue culture polystyrene trays with their deposited ECM and preserved cell-cell and cell-ECM interactions. PNIPAAm switches its properties reversibly between hydrophobic (cell adhesive) and hydrophilic (non-cell adhesive) states at temperatures higher and lower than its lower critical solution temperature (LCST) (~32°C) respectively [5]. Advances were recently made in the area of regenerative medicine where stacking of homotypic or heterotypic cell sheets onto patterned surfaces has shown the formation of functional 3D tissues and organ-like constructs [6].

PNIPAAm monolayer cell culturing is a promising tool for engineering tissue but the current technology is essentially based on the use of flat 2D substrates. The latter lacks structural and

organisational cues for cells since the 2D environment does not replicate the complexity of physiological tissue [7]. Where layered or patterned co-culture cell sheets are used, the process requires multiple steps and does not address the need for a structural matrix to enable cell growth in three dimensions. In recent years, some 3D PNIPAAm scaffolds have been developed based on hydrogels, grafted porous 3D membranes and micro-textured PNIPAAm surfaces [7,8]. Additionally a PP-*g*-PNIPAAm non-woven membrane with adsorbed antibodies has recently been reported in the literature for selective cell separation and enrichment of target cells [9]. However, to date little work has been done regarding applying the PNIPAAm technology to highly porous 3D scaffolds for the purpose of 3D cell propagation and non-invasive recovery of 3D cell constructs. Additionally many of these studies still focus on the formation of 2D cell monolayers for the purpose of tissue engineering and regenerative medicine. Recently, we have published the first report on non-invasive release of hepatocytes in 3D clusters using highly porous PNIPAAm grafted NWF [10].

Techniques reported in literature to graft PNIPAAm onto polymer surfaces include electron-beam radiation, gamma radiation, plasma radiation; UV-irradiation; ozonation; corona-discharge; chemical treatment, and controlled radical polymerisation techniques [11-13]. A key aspect for polymer graft polymerisation is surface functionalisation. Direct fluorination, i.e. treatment of a polymer with an elemental fluorine containing gas mixture, is an attractive alternative functionalisation method which can be used to modify polymer surfaces without changing the bulk properties [14]. When carried out in the presence of oxygen in the reaction vessel the process is referred to as “oxyfluorination”.

Oxyfluorination is known to form reactive polar groups on polymer surfaces, which can serve as active centres for grafting [15-16]. Oxyfluorination is less invasive compared to radiation, it is a dry technology, it can be used to modify substrates of any shape, it displays relatively

large surface penetration depths (~ 10 μm) and the treatment can be conducted at room temperature [14]. The formation of reactive peroxide groups (ROOH; ROOR) and long-lived trapped peroxy radicals (ROO•) on oxyfluorinated polymer surfaces is well-known [14, 17-18]. Direct fluorination and oxyfluorination treatments have been widely studied and applied commercially for barrier, adhesion, and printability properties of polymer substrates [14]. However, to our knowledge the use of oxyfluorination as a pre-treatment for graft polymerisation is not widely practised. Jeong *et al* [17] recently introduced the term "oxyfluorination-assisted graft polymerisation" (OAGP) technique to describe this facile two step process.

In this paper, we report on the synthesis of a novel PP-*g*-PNIPAAm NWF which was prepared using the OAGP method for use in 3D non-invasive cell culture. PP was chosen for the scaffold backbone material since it is relatively inexpensive; it can be easily converted into fibers using an extrusion process, and it displays chemical resistance and good mechanical properties. A NWF was chosen for the 3D matrix due to its highly permeable open 3D structure, large surface area; and high porosity whereby the pores would allow for sufficient cell-cell interactions while enabling diffusion of nutrients and oxygen to the cells.
The OAGP method involved :1) functionalisation of the virgin PP NWF(pNWF) with polar groups using oxyfluorination to produce oxyfluorinated NWF (oNWF) with improved wetting in an aqueous medium; and 2) graft polymerisation of the oNWF in an aqueous NIPAAm solution using ammonium persulphate (APS) as the initiator to produce the grafted NWF (gNWF). The chemical and physical properties of pNWF, oNWF, and gNWF were characterised using ATR-FTIR, SXPS, static water contact angle, X-ray diffraction (XRD), differential scanning calorimetry (DSC), and SEM. Finally, we demonstrate 3D cell culture using the gNWF in a bioreactor and show non-destructive temperature-induced release of hepatocyte cells.

2. Experimental Section

2.1. Preparation of pNWF

PP fibres of 6.7 dtex/60 mm were purchased from FiberVision (Denmark) and were processed into the NWF by a needle-punching technology as described previously [19]. The PP fibres were opened and needling was conducted from 2 sides using a needling depth of 6 mm. A capillary flow porometer was employed to determine the pore size distribution and the mean flow pores according to the 6212005-134 test of the ASTM E 1294 method. The total surface area of the pNWF (A_{NWF}) was calculated using the following equation: $A_{NWF} = \frac{4V_{NWF}}{d_{fibre}}$,

Where d_{fibre} refers to the average diameter of the fibre's used; and V_{NWF} is the volume of the pNWF which was calculated using the mean area weight of the NWF (g/m^2) and the density of PP which was taken as 0.903 g/cm^3.

2.2. Oxyfluorination of pNWF

Washed pNWF was oxyfluorinated at Pelchem (Pty) Ltd (SA) by a proprietary method [20]. The NWF was loaded into a Reaction Vessel (RV). The RV was purged with air and partially evacuated, and then a 20:80 F_2:N_2 gas mixture was introduced to allow the oxyfluorination reaction to proceed. The gas mixture was then cycle purged from the RV with air at 25 kPa to complete the oxyfluorination process. Hydrolysis post-treatment of the oNWF was investigated by incubating the oNWF in water at 23°C for 3 h, and at 70°C for 10 min. The hydrolysed oNWF samples were then dried and evaluated by ATR-FTIR.

2.3. Polymerisation of NIPAAm onto oNWF

Aqueous solutions of 10 wt% *N*-isopropylacrylamide (NIPAAm - Sigma Aldrich, 97%) and 10 wt% APS (Sigma Aldrich, >98%, ACS reagent) were prepared in deionised water. The oNWF was cut into disks (1.5 cm x 0.7 mm) and immersed in the APS solution and left to

swell to saturation for 16 h. Prior to grafting, the solutions were degassed for 30 minutes by continuously flowing high purity argon gas into the reaction vessels. The initiator solution was then immediately decanted, and a degassed solution of NIPAAm was added into each reaction vessel. Radical graft polymerisation was conducted in sealed vessels in an oil bath at 70^{o}C for 7 h. The gNWF was washed in copious amounts of cold deionised water for 72 h with regular water changes to remove PNIPAAm homopolymer or residual monomer and thereafter the gNWF was dried in an oven under vacuum at 50°C.

2.4. Chemical and physical composition analysis

To investigate the physiochemical changes occurring on the NWF, we conducted ATR-FTIR, SXPS, SEM, and XRD. For ATR-FTIR analysis, a Spectrum 100 FTIR spectrometer was used, with a diamond crystal and an average of 8 spots were taken per sample to get representative data. SXPS data were obtained using a Quantum2000 (Physical Electronic) SXPS equipped with an Al Kα(1486 eV) X-ray source (20 W), and a beam diameter of 100 µm. For SEM analysis, a LEO 1525 field emission SEM with Oxford's INCA system was used and samples were carbon sputtered. An X'PertPro wide angle XRD system was used to determine the crystal structure of the NWF's. A Ni filtered CuKα source was used with radiation of λ= 0.154 nm, with operating conditions of 40 mA, 45 kV, and exposure time of 12 minutes. Graft yield (in µg/cm^2) was determined using peak intensities of $I_{1644\ cm\text{-}1}$: $I_{1455\ cm\text{-}1}$ from the ATR-FTIR spectra. The graft thickness was estimated assuming a PNIPAAm density of 1.1 g/cm^3.

2.5. Contact angle

The static contact angles of pNWF, oNWF and gNWF were determined with a Kruss DSA 100. 4 µl of pure deionised water was dispensed onto the surface of the NWF using a dosing needle. The static contact angle was measured using image software based on the Young Laplace model. The contact angle was measured every second with a total drop age of 10

seconds using either circle or sessile-drop fitting, at 20°C and 40°C. For the latter, the NWF was equilibrated at 40°C in an oven for 1 h prior to analysis.

2.6. Thermal transitions of the NWF by DSC

To measure thermal transitions in the NWF, a DSC-Q2000 instrument and a MicroDSCIII apparatus (SETARAM) were used. For determining the melting and crystallisation peaks, dry samples were prepared and heated from -60°C to 250°C at a cycle of 20°C/min under N_2 gas using the DSC-Q2000. The degree of crystallisation was estimated from the heat of fusion measurements according to: % Crystallisation = ($\Delta Hf^*/\Delta Hf$) * 100, where ΔHf^* is the measured heat of fusion of the sample; and ΔHf is the heat of fusion of 100% PP, which was taken as 146.5 J/g [21]. For determining the LCST on the gNWF, 20 mg of dry grafted sample was placed in contact with 500 µL of deionised water and kept at 10°C for 2 h to obtain equilibrium [22]. Samples were heated from 0°C to 80°C at a heating rate of 0.5°C / min.

2.7. Temperature-induced cell release from the gNWF

The gNWF was cut into disks (15mm in diameter) which were ethanol sterilised. Three disks were stacked horizontally in an axial flow bioreactor and 4.5 x 10^6 HepG2 (ATCC HB-8065™, ATCC®) hepatocytes were seeded into the bioreactor via the sampling port. The cells were then allowed to settle and attach to the gNWF disks for 3 h. Dulbecco's Modified Eagle Medium (DMEM, Lonza Walkersville, Inc. Maryland, USA) with 2 mM L^{-1} glutamine and supplemented with 10% (v/v) foetal calf serum (FCS), 100 $g.mL^{-1}$ penicillin and 10 $\mu g.mL^{-1}$ streptomycin (Sigma-Aldrich Chemie, GmbH, Steinheim, Germany) was perfused into the bioreactor at 2 mL min^{-1} for a period of 10 days. A bioreactor running in parallel containing the pNWF was used as the control. To ascertain thermal release potential of the gNWF, the bioreactor was perfused with cold media at 20°C for 2 h. The media containing the released cells was then drained from the bioreactor, and the cells on the gNWF (before and after

thermal release) were stained with fluorescein diacetate (FDA) and visualised at 40x magnification using a standard fluorescence microscope (Olympus BX41) equipped with a 490 nm bandpass filter with a 510 nm cut-off filter for fluorescence emission. To ascertain if high-density cell culture was possible on the 3D NWF in the bioreactor, a preliminary trial was performed and cells were cultured for 14 days in the bioreactor as indicated above but at day 14 the media was drained and the NWF disks containing the proliferated cells were gently removed from the bioreactor, and the disks were trypsinated and the cells were harvested and counted using tryphan blue dye exclusion on a haemocytometer.

3. Results and Discussion

3.1. NWF manufacture

In this study, a 3D pNWF was developed for cell culture using a needle-punching technology, and the pNWF was grafted with PNIPAAm using an OAGP method. Using the needle-punching technique, highly porous pNWF was produced with a mean area weight of 100 g/m^2 and an average thickness of 3.3 mm. Capillary flow porometry indicated that the pNWF displayed mean flow pore diameters of 199.38 μm with minimum and maximum pore sizes of 7.68 μm and 411.09 μm respectively. The mean flow pores is a measure of liquid permeability of the scaffold, and was found to be highly dependent on the fibre specific surface area, and the machine processing parameters used. The total surface area of the pNWF was calculated to be ~1440 cm^2/g, indicating a relatively large surface area for cell growth.

3.2. Graft polymerisation method

The OAGP method proceeds via a free-radical chain mechanism which is diffusion driven and the possible reaction mechanism is shown in **Scheme 1**. During oxyfluorination the fluorine/oxygen (or air) gas mixture reacts exothermically with the surface of the pNWF to form free radicals [23]. Fluorine, due to its high electronegativity, partially replaces the

hydrogen on the polymer backbone to form alkyl free radicals (R•), fluorine free radicals (F•), as well as hydrogen fluoride [18]. Initiation via dissociation of molecular fluorine is not possible since homolysis of fluorine is too endothermic (ΔH = 155 kJ/mol) to proceed at room or relatively low temperatures [24]. The formed alkyl and fluoride free radicals then react to form the fluorocarbon backbone (CHF). Substitution of C-H bonds by C-F is preferential due to the higher bond energy of the latter [14]. It has been reported that in the presence of oxygen, acid fluorides, carboxylic acids, peroxy radicals (RO_2•) and peroxide groups (ROOH, ROOR) form on the oxyfluorinated surface [14,17,25]. According to Tu *et al* [26], oxidation of PP during oxyfluorination preferably occurs at the pendant methyl group. Using electron-spin resonance we have previously detected asymmetric singlet spectra confirming the presence of mid-chain peroxy radicals on the oNWF [27]. It has also been reported that trapped peroxy radicals undergo migration and decay by abstraction of H to form hydroperoxide (ROOH) as the primary oxidation product as shown in scheme 1, and peroxides can also form by recombination of two peroxy radicals (ROOR) [28]. At elevated temperatures, the peroxide on the PP backbone is homolytically cleaved due to the low bond dissociation energy of the O-O bond to form alkoxy radicals (RO•) [29]. Conversely the APS initiator, which is also a peroxide, undergoes thermal decomposition to form sulphate radical ions (SO_4•-) and hydroxyl radicals (OH•), which are capable of initiating polymerisation by adding to the unsaturated double bond of the NIPAAm monomer [30]. Finally, grafting of PNIPAAm onto the oNWF proceeds via coupling of the free radicals between the alkoxy radical (RO•) on the oNWF and the propagating chain of NIPAAm.

An advantage of the OAGP method used here is that toxic solvents were not required, and graft polymerisation was carried out in an aqueous medium under mild conditions. A further advantage with this method was that the NWF was swollen in the APS initiator solution such that the initiator molecules were localised on the fibres, so as to promote graft polymerisation

rather than homopolymerisation. However, due to the high water solubility of APS, some homopolymerisation occurred which was evident from the increased opacity of the medium as the reaction progressed. It is known that graft polymerisation is highly dependent on the monomer permeability into the polymer bulk, and monomer availability to the graft sites [31]. This was enabled by ensuring that the oNWF was highly swollen prior to grafting to ensure diffusion of the monomer molecules into the amorphous regions of the PP.

Grafting was conducted at 70°C, i.e. > LCST of PNIPAAm, at which temperature PNIPAAm is hydrophobic, and hence will preferentially precipitate on the PP matrix rather than remain in solution which may also contribute to increasing the graft yield on the PP surface.

3.3. Chemical composition of NWF

The chemical composition of pNWF, oNWF, and gNWF was studied by ATR-FTIR as shown in **Fig. 1**. After oxyfluorination, new absorption bands appeared on the oNWF at 3700-3000 cm^{-1}, 1736 cm^{-1}, and 900 cm^{-1} - 1300 cm^{-1} which were attributed to the O-H; C=O and C-F stretching vibrations respectively [32]. After graft polymerisation, characteristic PNIPAAm FTIR absorption bands at 3300 cm^{-1}; 1529 cm^{-1}; and 1639 cm^{-1} were observed for the gNWF corresponding to the broad amide II (N-H) stretch, amide II deformation and amide I (C=O) stretching vibration respectively. The graft yield was determined using $I_{1644\ cm\text{-}1}$: $I_{1455\ cm\text{-}1}$ from the ATR-FTIR spectra. Based on the peak area ratios, a graft yield of 24 ± 4 $\mu g/cm^2$ was obtained which corresponded to a graft thickness of 220 ± 38 nm, which indicates that the gNWF surface was covered by several monolayers of PNIPAAm.

Hydrolysis post-treatment revealed a decrease in peak intensities of the newly formed oxyfluorinated functional groups on the oNWF as shown in Fig. 1 (b-c), when hydrolysis was carried out at both room temperature and at elevated temperatures. Changes were observed to

all of the newly formed groups, i.e. O-H, C=O and the C-F groups. The lower ATR-FTIR peak intensities after the direct hydrolysis post-treatment of the oNWF can be attributed to a reduction in the Lewis basicity of the oxyfluorinated PP surface following hydrolysis due to conversion of the pure carbonyl group of the acid fluoride to carboxylic acid [26]. According to Tu *et al*, an inter-hydrogen bonded conjugated structure occurs in oxyfluorinated PP between two neighbouring COOH groups. This inter-hydrogen bonded structure could likely reduce the net dipole on the carbonyl peak and neighbouring C-F peaks, which would account for the reduced peak intensities of the newly formed oxyfluorinated groups after hydrolysis. Additionally after hydrolysis, a shoulder peak at ~1623 cm^{-1} grew in magnitude. A new functionality in the range of 1620-1623 cm^{-1} was also reported by Kharitonov *et al* following hydrolysis of oxyfluorinated LDPE which was attributed to C=O vibration in the enol form of the β-diketone or the double bond C=C stretching vibration (e.g. FC=CH) [14].

The SXPS studies (**Fig. 2 and Table 1**) obtained for the nascent and modified NWF corroborated with the ATR-FTIR data. From the C1s spectra, only one symmetric peak was measured for the pNWF at 284.8 eV (with 100% peak area), which represents the C-H of the PP backbone [32]. On the pNWF, ~4.2 at% of elemental oxygen was detected from the O1s spectra at 532.2 eV. The presence of a small amount of oxygen on pure PP was reported previously and was attributed to the impurities incorporated in PP as a result of some degradation occurring during processing in air [33]. The C1s spectra of the oNWF was asymmetrical and fitted with multiple peaks as follows (with the peak area % indicated in brackets): 284.7 eV (C-H: 63.12 %); 286.4 eV (C-OH, C-O-C:14.95%); 287.8 eV (CHF-CHF, CHF-CF_2: 13.45%), and 288.9 eV (C=O : 8.49%) [25,32]. The high-resolution O1s and F1s spectra for the oNWF showed single peaks at 533.3 eV and 687.4 eV which were assigned to the presence of C-O, and C-F respectively [25]. An O/F ratio of ~1 was observed (Table 1) on the oNWF surface, indicating that an equal amount of F and O atoms were present after

oxyfluorination, which was interesting since the oxygen present in the reactor during the treatment was mainly from air which was introduced during both the partial evacuation and the cycle purging steps. For the gNWF, the C1s, O1s, and N1s SXPS data confirmed the amide groups with peak assignment as follows: C1s: 284.8 eV (CH_3, CH_2,CH: 71.47%); 286.5 eV (CH-NH: 18.06%); 287.9 eV (C=O: 10.47; O1s: 531.2 eV (C=O:100%) and 399,6 eV (N-H:100%) respectively [34].

The degree of grafting was estimated from SXPS based on the N atomic concentration present on the grafted surface as compared to the theoretical N atomic content in PNIPAAm (Table 1)[34]. Considering that the oNWF displayed 1.4 at% N, the N content in the gNWF was corrected to 9 at%, correlating to a degree of grafting of 72.0% indicating that in the gNWF, ~72% of the surface was covered by PNIPAAm chains.

3.4. Contact angle

Contact angle measurements are routinely used to characterise the wettability and surface energy of materials. **Fig. 3** shows the measured water contact angles on the pNWF, oNWF, and gNWF over an ageing period of 10 seconds. The pNWF as expected displayed an intrinsically hydrophobic surface with a relatively stable water contact angle at ~ 135 ± 6° at 20°C, while for the oNWF the contact angle was reduced to ~ 127 ± 3° at 20°C. For the gNWF, a stable water drop could not be obtained due to the rapid wetting of water with the surface graft layer. The contact angle for the gNWF was found to be temperature-dependent showing a relatively hydrophobic surface at 40°C with improved hydrophilicity at 20°C, confirming the presence of PNIPAAm in the graft layer. The contact angles for both the pNWF and the oNWF did not vary with temperature and similar contact angle values were obtained at 20°C and at 40°C (data not shown). Although the contact angle measurements for the oNWF decreased compared to pNWF at 20°C, the small decrease in contact angle was

unexpected, and somewhat contradictory to the ATR-FTIR and SXPS data. Authors previously have reported relatively low contact angles for oxyfluorinated PP which is associated with increased wetting and hydrophilicity [32]. Our results for the contact angle cannot be directly compared to other studies due to the difference in the oxyfluorination conditions used, and the scaffold morphology. The NWF used in this study is highly porous, and it is known that porous surfaces are non-ideal for contact angle measurements using the Young equation due to the heterogeneity, roughness, capillary forces within pores, contraction of the polymer in the dry state, and restructuring of the surfaces [35]. However, comparison between samples can still be effectively made. A possible explanation for the relatively low decrease in contact angle of the oNWF compared to pNWF may be due to a surface rearrangement process of the oNWF. Hruska *et al* [36] have reported that the contact angle and surface energy of oxyfluorinated PP increases significantly with storage time due to re-orientation of the new polar functional groups away from the polymer surface into the polymer bulk in order to minimise the interfacial free energy at the surface. Since freshly oxyfluorinated NWF was unavailable during the contact angle studies, aged oNWF which had being stored for several months were used, hence surface restructuring is highly possible. It should also be noted that contact angle provides information about the outermost 5-10 Å of a solid surface. Thus, although the contact angle of oNWF was relatively similar to that of pNWF, the oxygen functionality is still present in the oxyfluorinated surface as we have confirmed by ATR-FTIR and SXPS. Furthermore re-orientation of functional groups was not observed for the gNWF which can be attributed to restricted mobility of the grafted PNIPAAm chains in the surface layer. Further work is needed to investigate the surface rearrangement process in the oNWF.

3.5. XRD and DSC studies

According to the XRD pattern as shown in **Fig. 4**, the PP in the pNWF crystallized in the α-monoclinic form showing a characteristic diffractogram of isotactic PP [37]. From Figure 5, it can be seen that PNIPAAm is completely amorphous. The oNWF and gNWF both showed a similar diffractogram to that of the pNWF, indicating that after OAGP the arrangement of the atoms in the crystal lattice remained in the α-monoclinic form. However from the DSC analysis changes were observed for both the crystallisation and melting peaks of the pNWF compared to the oNWF and gNWF (**Fig. 5** a-b). A sharp symmetric crystallisation peak was observed for the pNWF at Tc_{max} of 111.6 °C indicating a relatively pure semi-crystalline material, however for the oNWF and the gNWF, the crystallisation peaks appeared somewhat broader, and was shifted to higher temperatures (Tc_{max}117.7 °C and 115.1 °C respectively) compared to the pNWF. Furthermore the pNWF showed a single melting peak at 161.1 °C indicating one stable crystalline form in PP, while for oNWF and gNWF twin melting peaks were observed in both cases at T_{m1}:147.2 °C and T_{m2}:161.6 °C; and at T_{m1}:148.57°C and T_{m2}:165.22°C respectively. Twin melting peaks was observed previously for isotactic PP and can be attributed to a combination of imperfect crystals that are less stable and that would melt first, and pure well-ordered PP crystals that melt at a higher temperature [21,37]. Additionally crystals of different sizes may be present due to the modification, which would melt at different rates. The degree of crystallinity of the pNWF was found to be 52.8 % indicating a semi-crystalline material. After oxyfluorination and grafting, the crystallisation percent of the NWF decreased to 48.2 % and 45.1 % respectively indicating that OAGP resulted in only a slight reduction in the cystallinity of PP. It can be assumed that some crystal defects are located in the peripheral zones of the crystallites, with the majority contained in the amorphous regions. DSC was also conducted on wet gNWF as shown in Fig. 5c. A LCST was detected at Tp of 33.4 °C which further confirmed the presence of PNIPAAm in the gNWF, and also indicated that the OAGP method did not modify the LCST of PNIPAAm.

3.6. Surface morphology from scanning electron microscopy

From SEM the fibres contained in the pNWF displayed a smooth surface texture as shown in **Fig. 6** a. However some artefacts were observed on the surface of the pNWF, which could be the result of the nonwoven manufacturing process. After oxyfluorination, the surface contained numerous "cracks" (Fig. 6b) which appeared to run across the fibre length and the surface displayed increased roughness compared to the control. Increased surface roughness was also noticed by Kranz *et al* [33] during oxyfluorination of PP and PE. After graft polymerisation (Fig. 6c-d), the PNIPAAm layer could be detected on the surface of the gNWF and the architecture of the nonwoven matrix was retained, with changes only observed to the fibre surface. This was of particular importance since the gNWF should retain its open porous structure to enable efficient 3D cell culturing.

3.7. Temperature-induced cell release

We have recently demonstrated temperature-triggered cell release from PNIPAAm grafted NWF (including nylon, poly(ethyleneterephthalate) and PP) in static culture and also reported on cell proliferation, morphology, albumin production, and gene expression of hepatocytes cultured on the grafted NWF[10]. In this work, we investigated temperature-triggered cell release when cells were cultured on gNWF disks in a bioreactor, where high-density cell culture is possible. Hepatocytes were seeded on three gNWF disks and cultured for 10 days in the bioreactor to determine non-destructive cell release at 20°C. To determine cell viability, cells were stained with fluorescein diacetate, which is essentially converted into fluorescein, a green fluorescent compound, by viable cells only [38]. **Fig. 7** a shows hepatocyte cells on a gNWF disk at 37°C at day 10 in culture while Fig.7 (b-c) show cells remaining on the gNWF and pNWF disks respectively after temperature-induced cell release at 20°C. Cells remained viable on both the pNWF and the gNWF after 10 days in culture in the bioreactor. A significant amount of cells were released from the gNWF at 20°C compared to the pNWF

control), confirming the thermoresponsive behaviour of the gNWF. Only minimal cell release was seen from the pNWF disk at 20°C due to loose cells falling off the scaffold (Fig. 7c). It was observed that not all the cells were released from the gNWF with a temperature change. This may possibly be attributed to inhomogeneity in the PNIPAAm layer on the gNWF surface. Interestingly the cells grown on the gNWF arranged themselves as 3D multicellular aggregates (Fig. 7a), which we have also reported previously [10]. 3D cell aggregates are more representative of physiological tissue in terms of morphology and function, as opposed to monolayer cell sheets thereby providing a more physiological relevant *in vitro* model for cell culture [2]. Additionally 3D cultures of hepatocytes are of particular importance for maintaining liver-specific function which is essential for drug-screening applications [2].

A preliminary trial was conducted to ascertain if high-density cell culture was possible in the bioreactor. A total of 4.5 $x10^6$ cells were initially seeded into the bioreactor containing three stacked pNWF disks (15mm diameter), and 39.7 x 10^6 and 49.9 x 10^6 hepatocytes were harvested from the bioreactor in two independent experiments at day 14, representing a 10 fold increase in cell numbers. This preliminary study indicates that high density cell culture is possible on the NWF in the bioreactor, however further studies are now ongoing to verify high-density cell culture using the gNWF disks.

4. Conclusion

In this communication we described the synthesis of highly porous 3D PP-*g*-PNIPAAm NWF using a facile method based on OAGP. We showed that OAGP can be effectively used to firstly functionalise non-polar and highly hydrophobic PP surfaces with reactive polar groups, as well as enable graft polymerisation of NIPAAm in aqueous medium without requiring toxic solvents. A free radical mechanism was proposed for the OAGP method with initiation

via SO_4•-; OH• and RO• radicals. This method presents an attractive alternative to other more expensive graft polymerisation technologies such as gamma radiation, plasma-radiation etc. Finally we showed temperature-triggered cell release from a bioreactor whereby viable and confluent cells were released spontaneously and non-destructively from the surface of the gNWF by cooling the cell culture medium from 37°C to 20°C, and without requiring destructive enzymes. The gNWF is highly porous and allows cells to easily attach and proliferate in 3D constructs in the pores of the scaffold which provides a more relevant *in vivo* model for cells. We have also showed that high-density cell culture on the NWF is possible in the bioreactor due to the large surface area of the NWF and the ease of stacking of multiple scaffolds for high through-put cell culturing. Further improvements are required with respect to optimisation of the graft homogeneity on the NWF surface. This will likely contribute to further improving the efficiency of the cell release process from the gNWF. The thermoresponsive gNWF of the present study could potentially be used for a large number of applications where intact 3D cells are required such as drug screening of new drug-leads, cytotoxicity assays, cancer research, stem cell research, and tissue engineering.

Acknowledgements

The authors acknowledge the CSIR, the NRF (Grant No. 61850) and the Hungarian National Office for Research and Technology (Grant ZA-9/2006) for funding this work. Pelchem Pty Ltd (SA) is thanked for oxyfluorination treatment of the nonwovens.

References

1] B.A. Justice, N.A. Badr, R.A. Felder, Drug Discovery Today 14 (2009) 102-107.

[2] F. Pampaloni, E.G. Reynaud, E. H. K. Stelzer, Nat. Rev. Mol. Cell. Biol. 8 (2007) 839-845.

[3] H. E. Canavan, X. Cheng, D. J. Graham, B. D. Ratner, D. G. Castner, J. Biomed. Mater. Res-A. 75 (2005) 1-13.

[4] O. Guillame-Gentil, O. Semenov, A. S. Roca, T. Groth, R. Zahn,J. Vörös, M. Zenobi-Wong, Adv. Mater. 22 (2010) 5443–5462.

[5] T. Okano, N. Yamada, M. Okuhara, H. Sakai, Y. Sakurai, Biomaterials 16 (1995) 297-303.

[6] J. Yang, M. Yamato, C. Kohno, A. Nishimoto, H. Sekine, F. Fukai, T. Okano, Biomaterials 26 (2005) 6415–6422.

[7] B. C. Isenberg, Y. Tsuda, C. Williams, T. Shimizu, M. Yamato, T. Okano, J. Y. Wong, Biomaterials 29 (2008) 2565–2572.

[8] I. K. Kwon, T. Matsuda, Biomaterials 27 (2006) 986–995.

[9] A. Okamura, T. Hagiwara, S. Yamagami, M. Yamaguchi, T. Shinbo, T. Kanamori, S. Kondo, K. Miwa, I. Itagaki, J. Biosci. Bioeng. 105 (2008) 221–225.

[10] C. L. Rossouw, A. S. Chetty, F. S. Moolman, L. M. Birkholtz, H. Hoppe, D. Mancama, Biotechnol Bioeng 109 (2012) 2147-2158.

[11] E. Bucio, G. A. E. Burillo, X. Coqueret, Macromol Mater Eng 290 (2005) 745-752.

[12] A. Contreras-Garcıa, G. Burillo, R. Aliev, E. Bucio, Radiat. Phys. Chem. 77 (2008) 936–940.

[13] L. S. Wan, Y. F. Yang, J. Tian, M. X. Hu, Z. K. Xu, J. Membr. Sci. 327 (2009) 174–181.

[14] A. P. Kharitonov, Prog. Org. Coat. 61 (2008) 192-204.

[15] A.P. Kharitonov, J. Fluorine Chem. 103 (2000) 123-127.

[16] A.P. Kharitonov, Yu.L. Moskvin, D.A. Syrtsova, V.M. Starov, V.V. Teplyakov, J. Appl. Polym. Sci. 92 (2004) 6-17.

[17] E. Jeong, T. S. Bae, S. M. Yun, S. W. Woo, Y. S. Lee, Colloids Surf., A. 373 (2011) 36-41.

[18] S. W. Woo, M. Y. Song, J. S. Rho, Y. S. Lee, J. Ind. Eng. Chem. 11 (2005) 55-61.

[19] L. Boguslavsky, FILTREX Germany (2010) ISBN 2-930159-70-7.

[20] ZA. PCT/IB03/0470 (2003), South Africa Nuclear Energy Corporation limited, invs.: I. d. V. Louw, P. A. B. Carstens.

[21] M. N. Huda, H. Dragaun, S. Bauer, H. Muschik, P. Skalicky, Colloid. Polym. Sci. 263 (1985) 730-737.

[22] K. László, K. Kosik, E. Geissler, Macromolecules 37 (2004) 10067-10072.

[23] F. J. du Toit, R. D. Sanderson, J. Fluorine Chem. 98 (1999) 107-114.

[24] W. A. Pryor, In Prentice-hall foundations of modern organic chemistry series, Prentice-Hall Inc. London, 1966, p 61.

[25] S. J. Park, S. Y. Song, J. S. Shin, J. M. Rhee, J. Colloid Interface Sci. 285 (2005) 190–195.

[26] L. Tu, D. Kruger, J. B. Wagener, P. A. B. Carstens, J. Adhes. 62 (1997) 187-211.

[27] V. Vargha, A. Chetty, Z. J. M. Sulyok, Z. Keresztes, I. Sajó, L. Korecz, R. Anandjiwala, L. Boguslavsky, J. Therm. Anal. Calorim. (2011) DOI 10.1007/s10973-011-1940-8.

[28] G. Geuskens, G. Nedelkos, Makromol. Chem. 194 (1993) 3349-3355.

[29] K. Kildal, K. Olafsen, A. Stori, J. Appl. Polym. Sci. 44 (1992) 1893-1898.

[30] I. P. Riggs, F. Rodriguez, J. Polym. Sci., Part A-1: Polym. Chem. 5 (1967) 3151-3165.

[31] N. Anjum, O. Moreau, A. M. Riquet, J. Appl. Polym. Sci. 100 (2006) 546–553.

[32] B. K. Lee, Y. S. Lee, Y. B. Chong, J. B. Choi, J. R. Rho, J. Ind. Eng. Chem. 9 (2003) 426-432.

[33] G. Kranz, R. Luschen, T. Gesang, V. Schlett, O. D. Hennemann, W. D. Stohrer, Int J Adhes. Adhes. 14 (1994) 243-253.

[34] Y. Akiyama, A. Kushida, M. Yamato, A. Kikuchi, T. Okano, J. Nanosci. Nanotechnol. 7 (2007) 796-802.

[35] R. Q. Kou, Z. K. Xu, H. T. Deng, Z. M. Liu, P. Seta, Y. Xu, Langmuir 19 (2003) 19, 6869-6875.

[36] Z. Hruska, X. Lepot, J. Fluorine Chem. 105 (2000) 87-93.

[37] Z. Horváth, I. E. Sajó, K. Stoll, A. Menyhárd, J. Varga, Express Polym. Lett. 4 (2010) 101–114.

[38] M. Dvir-Ginsberg, I. Gamlieli-Bonshtein, R. Agbaria, S. Cohen, Tissue Eng. 9 (2003) 757-766.

Table 1. C1s, N1s, O1s, and F1s atomic % for pNWF, oNWF, and gNWF by SXPS.

	Atomic [%]			
Substrate	**C1s**	**N1s**	**O1s**	**F1s**
pNWF	95.8	-	4.2	-
oNWF	62.5	1.4	18.2	17.9
gNWF	74.9	10.4	13.1	1.6
PNIPAAm (calculated)[32]	75.0	12.5	12.5	-

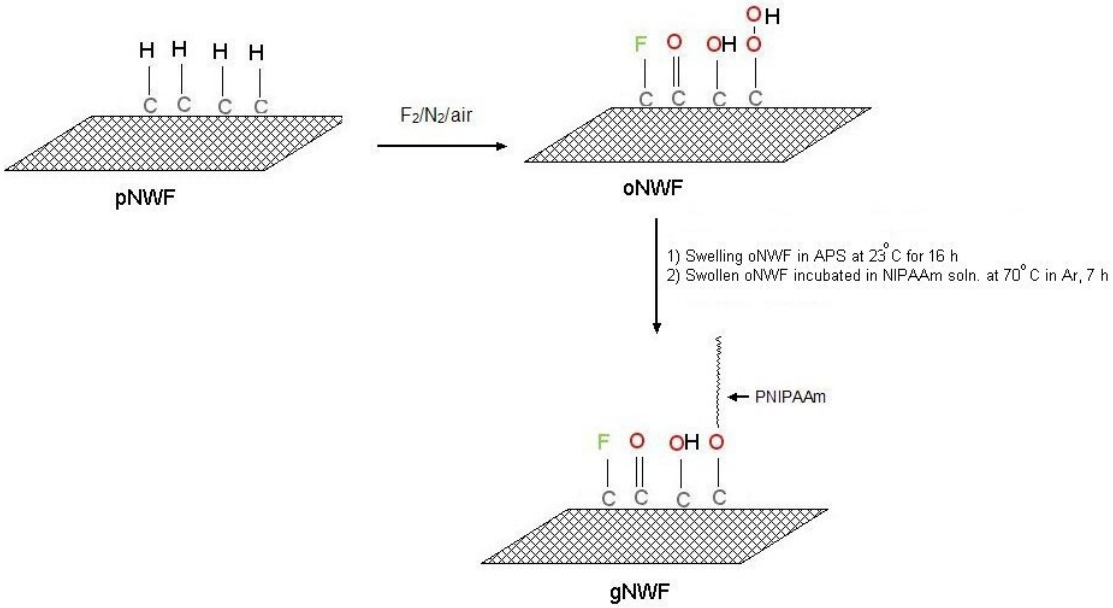

Scheme 1. Schematic representation showing the possible mechanism for OAGP of PNIPAAm onto PP.

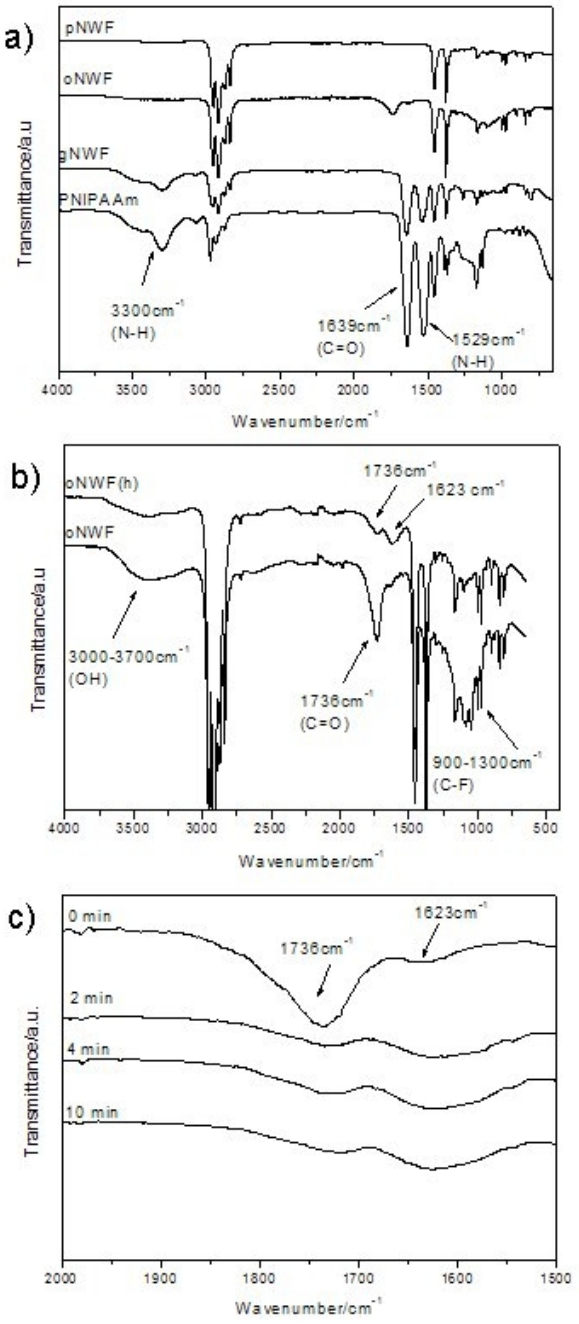

Fig. 1. ATR-FTIR spectra of a) pNWF, oNWF, gNWF and PNIPAAm homopolymer; b) oNWF before and after hydrolysis post-treatment (oNWF(h)) in water at 23°C for 3 h; and c) oNWF after hydrolysis post-treatment in water 70ºC from 0-10 min.

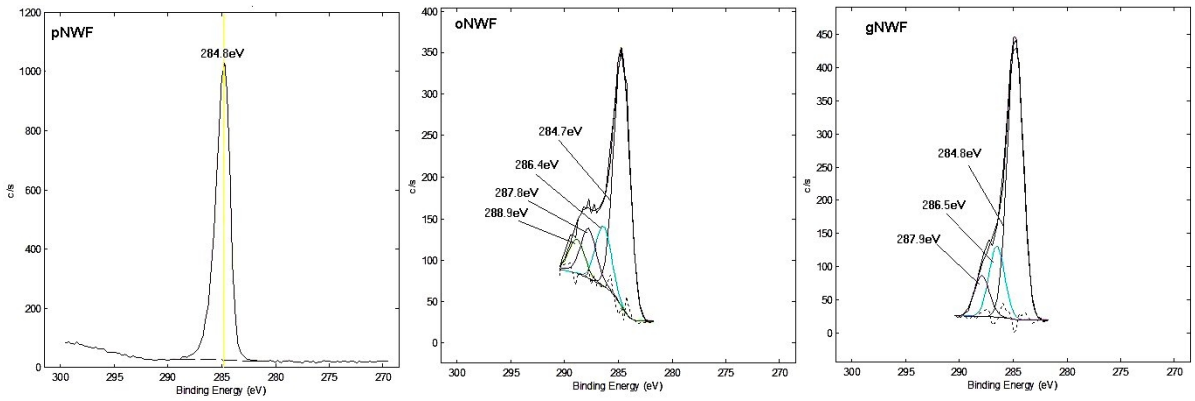

Fig. 2. C1s XPS spectra of pNWF; oNWF and gNWF.

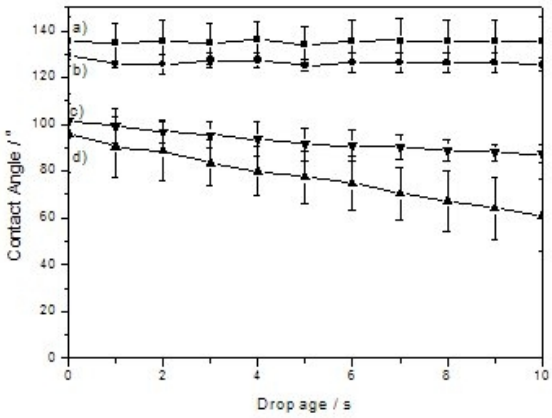

Fig. 3. Static water contact angle on the surface a) pNWF at 20 ^{o}C, b) oNWF at 20 ^{o}C, c) gNWF at 20 ^{o}C and d) gNWF at 40 ^{o}C as a function of the drop age. Three drops were aged per sample.

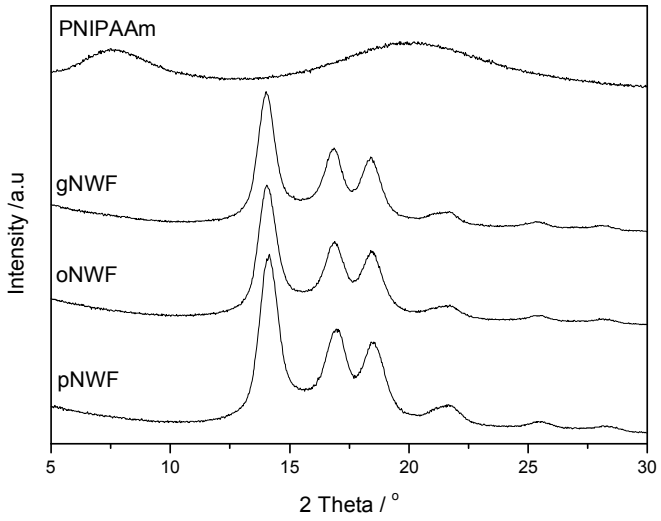

Fig. 4. XRD diffractograms of pNWF, oNWF, gNWF and PNIPAAm homopolymer (control).

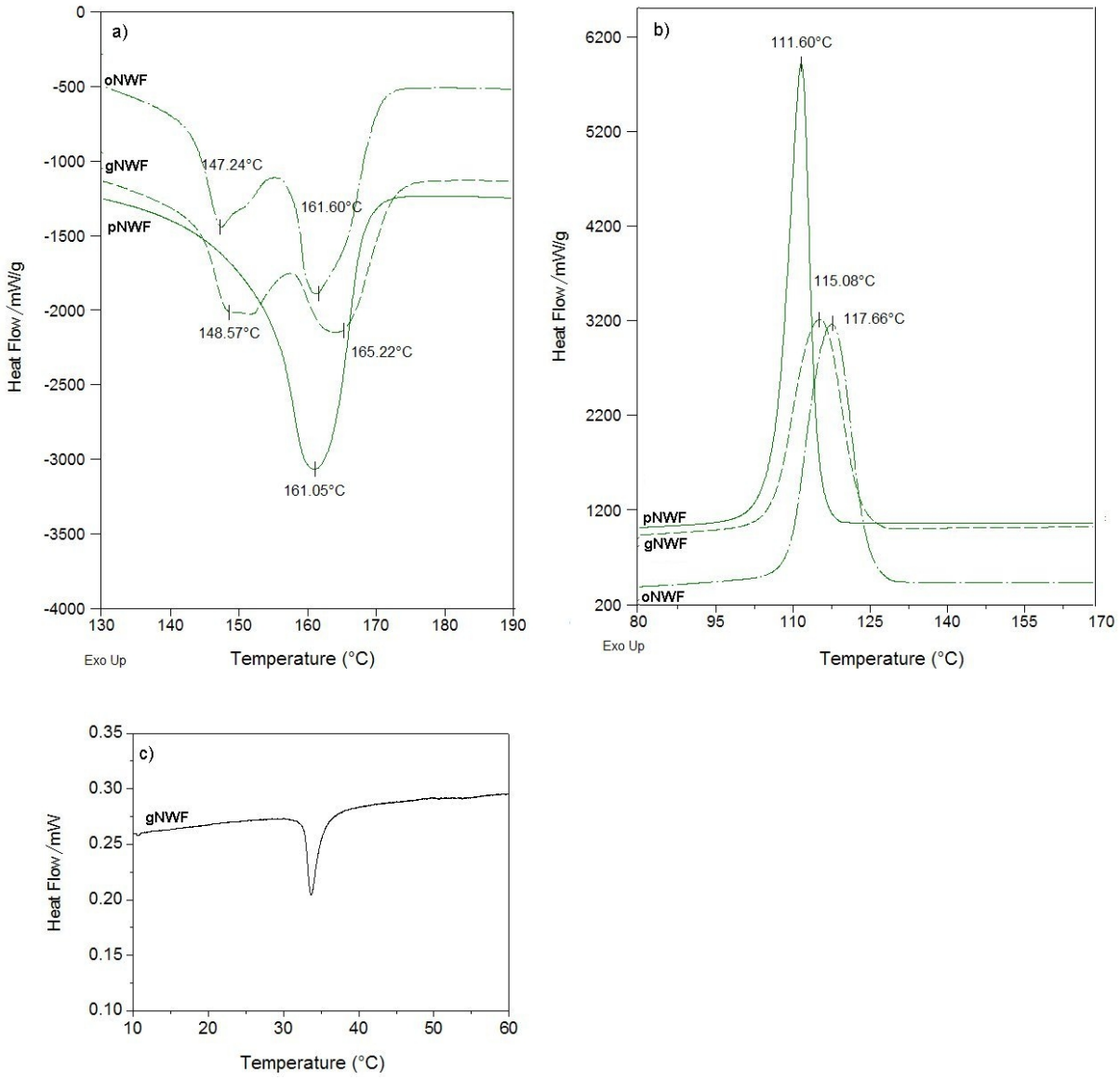

Fig. 5. a) 1st cooling DSC thermogram and b) 2nd heating DSC thermogram of pNWF, oNWF, and gNWF, and c) 2nd heating DSC thermogram of gNWF showing a LCST at ~33.4 °C using wet samples.

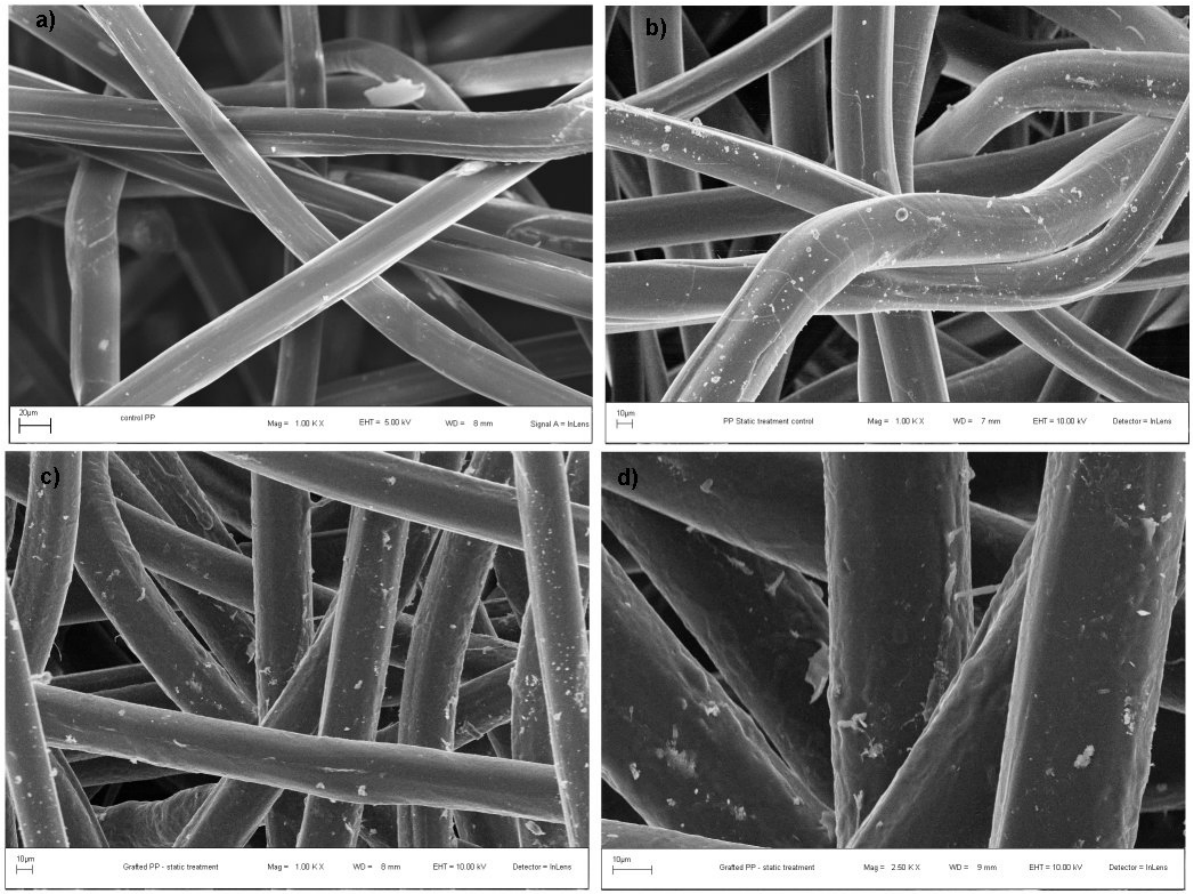

Fig. 6. SEM images of a) pNWF; b) oNWF; and c-d) gNWF.

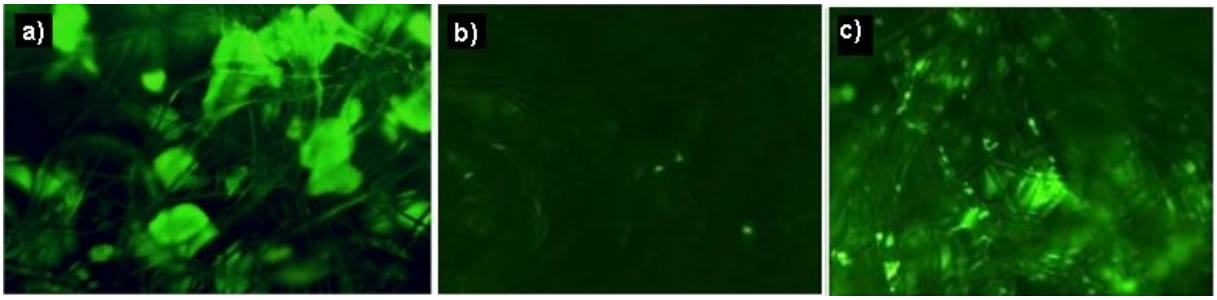

Fig. 7. HepG2 cells (a) growing on the gNWF scaffold in the bioreactor at 37°C for 10 days prior to thermal release; (b) cells remaining on the gNWF after thermal release from the bioreactor at 20°C for 2h; and (c) cells remaining on the pNWF (control) after thermal release from the bioreactor at 20°C for 2h.